

# Unique CD18 mutations involving a deletion in the extracellular stalk region and a major truncation of the cytoplasmic domain in a patient with leukocyte adhesion deficiency type 1

Patricia Hixson, C. Wayne Smith, Susan B. Shurin, and Michael F. Tosi

Two novel CD18 mutations were identified in a patient who was a compound heterozygote with type 1 leukocyte adhesion deficiency and whose phenotype was typical except that he exhibited hypertrophic scarring. A deletion of 36 nucleotides in exon 12 (1622del36) predicted the net loss of 12 amino acid (aa) residues in the third cysteine-rich repeat of the extracellular stalk region (mut-1). A nonsense mutation in exon 15 (2200G>T), predicted a 36-aa truncation of the cytoplasmic domain (mut-2). Lymphocyte function-

associated antigen 1 (LFA-1) and macrophage antigen-1 (Mac-1) containing the mut-1  $\beta_2$  subunit were expressed at very low levels compared with wild-type (wt)  $\beta_2$ . Mac-1 and LFA-1 expression with the mut-2  $\beta_2$  subunit were equivalent to results with wt  $\beta_2$ . Binding function of Mac-1 with mut-2  $\beta_2$  was equivalent to that with wt  $\beta_2$ . However, binding function of LFA-1 with the mut-2  $\beta_2$  subunit was reduced by 50% versus wt  $\beta_2$ . It was concluded that (1) the portion of the CD18 stalk region deleted in mut-1 is critical for  $\beta_2$  integrin

heterodimer expression but the portion of the cytoplasmic domain truncated in mut-2 is not; and (2) the mut-2 cytoplasmic domain truncation impairs binding function of LFA-1 but not of Mac-1. Studies with the patient's neutrophils (PMNs) were consistent with functional impairment of LFA-1 but not of Mac-1. (Blood. 2004;103:1105-1113)

© 2004 by The American Society of Hematology

## Introduction

Important insights related to the molecular mechanisms that determine  $\beta_2$  integrin structure and function have arisen from the study of naturally occurring mutations in the common  $\beta_2$  subunit of this integrin family.<sup>1,2</sup> A range of mutations in the CD18 gene have been identified in patients with leukocyte adhesion deficiency type 1 (LAD-1), including deletions, truncations, substitutions, frame shifts, and intronic mutations that result in abnormalities of the CD18 protein ranging from absence of protein product, deficient alpha-beta subunit association, and reduced protein size.<sup>1,3-5</sup> All such mutations have resulted in diminished expression of the CD18 integrins on leukocytes, and some mutations also have caused integrin dysfunction.<sup>1,3-5</sup> Patients typically have recurrent bacterial or fungal infections of skin and mucous membranes, impaired mobilization of leukocytes to sites of infection, severe gingivitis/periodontitis with permanent loss of dentition, and atrophic scarring of wounds.<sup>1,2,6</sup> Laboratory features include a pronounced leukocytosis in the absence of infection, reduced expression of all members of the CD18 or  $\beta_2$  integrin family on circulating leukocytes, and diminished CD18-dependent leukocyte functions, including cell adhesion, chemotaxis, transendothelial migration, and oxidative burst activation in response to iC3b-coated particles.<sup>1,2,6</sup>

We have identified an adult male patient with LAD-1 whose clinical features resemble those of the moderate LAD-1 phenotype, except that his wounds heal with hypertrophic rather than atrophic

scarring. His levels of CD18 integrin expression are higher than those of most other reported patients with the moderate phenotype of LAD-1, but the CD18-dependent functions of his leukocytes were similar to those of other moderate phenotype individuals.<sup>1,7</sup> He was found to be a compound heterozygote with 2 novel mutations, one of special interest in that it involves a major truncation of the cytoplasmic domain of CD18. Studies of COS-7 cells transfected with his mutant CD18 alleles and of his native leukocytes revealed distinct influences of his mutations on integrin expression and function. A quantitative relationship was established between the amount of macrophage antigen-1 (Mac-1) present at the neutrophil (PMN) surface, including translocated Mac-1, and the capacity of the PMNs for Mac-1-mediated adhesion induced by a subsequent optimal stimulus.

## Patients, materials, and methods

### Subject and controls

The patient is a 35-year-old man who was reported previously by Shurin et al<sup>8</sup> in 1979 as having a disorder of PMN chemotaxis presumed to be caused by the overgrowth in the oral cavity of *Capnocytophaga*, sonicates of which contained a dialyzable inhibitor of PMN chemotaxis. His clinical course to that time was characterized by early severe periodontal disease with loss of alveolar bone, persistent neutrophilia, and recurrent boils containing clear fluid. Over the last 20 years he has been generally healthy, except for

From the Department of Pediatrics, Section of Leukocyte Biology, Baylor College of Medicine, Houston, TX; and Department of Pediatrics, Case Western Reserve University School of Medicine, Cleveland, OH.

Submitted August 13, 2003; accepted September 22, 2003. Prepublished online as *Blood* First Edition Paper, September 25, 2003; DOI 10.1182/blood-2003-08-2780.

Supported by United States Public Health Service (USPHS) grants AI19031, AI45802, and HL42550.

**Reprints:** C. Wayne Smith, CNRC/Leukocyte Biology, 1100 Bates Ave, Suite 6014, Houston, TX 77030; e-mail: cwsmith@bcm.tmc.edu.

The publication costs of this article were defrayed in part by page charge payment. Therefore, and solely to indicate this fact, this article is hereby marked "advertisement" in accordance with 18 U.S.C. section 1734.

© 2004 by The American Society of Hematology

hypertrophic scarring of skin cuts and abrasions and 2 episodes of acute abdominal pain associated with terminal ileitis that resolved with intravenous antimicrobial therapy. He has had permanent dentures for over 25 years, and he has been relatively free of gingival symptoms. A more recent orolabial infection due to *Candida albicans* and peripheral blood PMN counts of more than  $20 \times 10^9/L$  ( $20\,000/\mu L$ ) for several weeks after successful treatment prompted a reevaluation of his PMN function. Because many aspects of this patient's clinical course were similar to those previously described for patients with the moderate phenotype of LAD-1,<sup>9</sup> a disorder not yet characterized when he was reported originally, subsequent laboratory evaluation focused on that disorder. Both parents and a 38-year-old sister, all in good health, were also studied. Healthy adult volunteers provided blood leukocytes for use as controls. Flow cytometric analysis of PMNs from the patient confirmed abnormally low expression levels of CD18 integrins.

### Monoclonal antibodies and other reagents

Monoclonal antibodies (mAbs) against CD11a included TS1/22 (provided by Dr Timothy Springer, Boston, MA) and R3.1 (provided by Robert Rothlein, Boehringer Ingelheim Pharmaceuticals, Ridgefield, CT); mAbs against CD11b included M1/70 (hybridoma clone purchased from American Type Culture Collection [ATCC], Manassas, VA), 60.1 (provided by John Harlan, Seattle, WA), and anti-Leu15 (Becton Dickinson, Mountain View, CA); mAbs against CD11c included anti-LeuM5 (Becton Dickinson); mAbs against CD18 included R15.7 (R. Rothlein), TS1/18 (T. Springer), and MHM23 (ATCC). Additional mAbs included anti-CD35 (CR1; clone 3D9, from Dr Melvin Berger, Cleveland, OH), anti-CD32 (Fc $\gamma$ R2, clone IV.3, from Dr Paul Guyre, Hanover, NH), anti-L-selectin (anti-Leu-8; Becton Dickinson), anti-E-selectin from clone CL2,<sup>9</sup> anti-CD3, anti-CD4, and anti-CD8 (OKT3, OKT4, OKT8, respectively; Ortho Diagnostics, Raritan, NJ). Some antibodies were used as direct fluorescent conjugates, where noted. Buffers and cell culture media were purchased from GIBCO Biologics (Grand Island, NY). Except as noted below, all other reagents were purchased from Sigma Chemical (St Louis, MO) or from Calbiochem-Behring (San Diego, CA).

### Isolation of PMNs and mononuclear cells from peripheral blood

PMNs and mononuclear cells were isolated from peripheral blood as previously described,<sup>10</sup> with minor modifications, using dextran sedimentation of erythrocytes and centrifugation of cells from the top leukocyte layer over a Ficoll-Hypaque cushion. Both the purity and viability of the pelleted PMNs prepared by this method were uniformly 95% or higher. For some studies, residual red blood cells in the pellet were removed by hypotonic lysis. Mononuclear cell fractions from the interphase layer were used to prepare immortalized B-lymphocyte lines by transformation with Epstein-Barr virus<sup>11</sup> (EBV) and as a source of cellular RNA.

### cDNA amplification

RNA was isolated from mononuclear leukocytes using TRIZOL Reagent (Invitrogen Life Technologies, Carlsbad, CA) and reverse transcribed using Moloney murine leukemia virus reverse transcriptase (Invitrogen), followed by amplification of the full-length CD18 cDNA as 4 overlapping fragments using the primers listed in Table 1. The polymerase chain reaction (PCR) conditions were as follows: one cycle at 95°C for 5 minutes followed by 35 cycles of 1 minute at 95°C, 1 minute at 58°C, 1 minute at 72°C, and a final step of 10 minutes at 72°C. The PCR products were electrophoresed on 1% agarose gels and purified with the QIAquick Gel Extraction Kit (QIAGEN, Valencia, CA). The purified fragments were sequenced by the Core Laboratory Services of the Children's Health Research Center (Department of Pediatrics, Baylor College of Medicine) using the 3100 Genetic Analyzer (Applied Biosystems, Foster City, CA).

### Subcloning and transformation

Full-length CD18 cDNA was obtained by ligating together the above PCR products that showed sequence integrity and then subcloned into the shuttle vector pCDNA3.1 (Invitrogen). The restriction sites for ligation were as

**Table 1. Primers used to amplify CD18 cDNA as 4 overlapping fragments**

Fragment	Primer sequence
1	
CD18/178F	5'- <u>ACT GGC GGC CGC</u> ATG CTG GGC CTG CGC CCC CCA-3'
CD18/784R	5'-CAA ACG GGG GCT GGC ACT CT-3'
2	
CD18/483F	5'-AGT GAC GCT TTA CCT GCG ACC A-3'
CD18/1188R	5'-GAT GAT CTC GGT GAG TTT CTC GTA G-3'
3	
CD18/1032F	5'-CTG TCA CCT GGA GGA CAA CTT GTA C-3'
CD18/1916R	5'-TCA GTG GTC CTC TCG CAC TG-3'
4	
CD18/1738F	5'-ACC AGC GAC GTC CCC GGC AA-3'
CD18/2487R	5'- <u>CAT GCT CGA GCT</u> AAC TCT CAG CAA ACT TGG G-3'

The numbering of nucleotides is based on sequence data provided by Weitzman et al,<sup>12</sup> with the initiating ATG beginning with A178. Underlined nucleotides in the primers for fragments 1 and 4 are *NotI* and *XhoI* linkers, respectively (boldface), plus 4 additional random nucleotides added to enhance product stability (plain type).

follows: *BglII* (T674/T675) for fragments 1 and 2; *EcoRI* (G1069/A1070) for fragments 2 and 3; and *AarII* (T1748/C1749) for fragments 3 and 4. The cDNAs encoding CD11a and CD11b, subcloned in the expression vectors pAPRM8 and pCDM8, respectively, were generous gifts from Dr T. Springer.

Bacteria of the electrocompetent *Escherichia coli* strain ElectroMAX DH5 $\alpha$ -E (Invitrogen) were transformed by electroporation using the Gene Pulser II System (Bio-Rad Laboratories, Hercules, CA) under conditions recommended by the vendor for this bacterial strain. The transformed bacteria were added to 1 mL room temperature SOC medium and shaken at 225 rpm for 1 hour at 37°C, serially diluted with SOC medium, and plated on Luria-Bertani (LB) agar plates containing 100  $\mu$ g/mL ampicillin.

### Plasmid preparation and cotransfection of COS-7 cells

Random bacterial colonies were selected and grown overnight at 37°C for small-scale plasmid preparation (QIAGEN Plasmid Mini Kit). After confirming the sequence integrity of CD18 cDNA inserts, large-scale plasmid preparation was performed using either the QIAGEN Plasmid Midi or Maxi Kit.

Transfection of COS-7 cells was carried out using Lipofectamine 2000 (Invitrogen) and performed according to the manufacturer's recommendations, using 5  $\mu$ g of CD11a or CD11b cDNA and 5  $\mu$ g of CD18 cDNA for each 25 cm<sup>2</sup> flask of COS-7 cells at about 90% confluence. The cells were incubated for an additional 48 hours to allow expression of the integrin constructs.

### Immunofluorescence flow cytometry for expression of CD11/CD18 molecules on COS-7 cells or blood leukocytes

Staining and analysis for direct immunofluorescence were performed for COS-7 cells as previously described.<sup>13</sup> Results were corrected for background fluorescence obtained with nonbinding isotype-matched mAbs. Leukocytes in whole blood also were stained with directly conjugated mAbs and analyzed in a FACScan (Becton Dickinson) flow cytometer, with gating of cells by 90° light scatter for granularity and forward light scatter for cell size to distinguish PMN, lymphocyte, or monocyte populations. For some studies, the chemoattractant N-formyl-methionyl-leucyl-phenylalanine (fMLF) was added at concentrations up to 10 nM for 20 minutes at 37°C to partially or fully up-regulate PMN surface expression of CD11b/CD18 prior to staining. Results were corrected for background fluorescence. Estimation of the number of Mac-1 surface sites on PMNs was achieved using a calibrated set of antibody-bound bead standards, as previously described.<sup>14</sup> For blood lymphocyte populations, 2-color fluorescence was used, with gating achieved using a fluorescein isothiocyanate (FITC)-conjugated population marker (anti-CD3, anti-CD4, or anti-CD8) and CD18 or a phycoerythrin (PE)-conjugated mAb for CD11a expression.

### Northern transfer and hybridization

Total RNA was extracted from transfected COS-7 cells using TRIZOL Reagent (Invitrogen). RNA (10  $\mu$ g) was loaded onto agarose gels containing formaldehyde, electrophoresed, and transferred to nylon membranes (GeneScreen Plus; PerkinElmer Life Sciences, Boston, MA), which were then baked at 80°C for 1 hour in a vacuum oven. CD18 fragment 2 cDNA (see Table 1) was used as a probe for CD18 message. The labeled probe was prepared with the Prime-It II Random Primer Labeling Kit (Stratagene Cloning Systems, La Jolla, CA) according to the manufacturer's protocol. After a 30-minute prehybridization with ULTRAhyb (Ambion, Austin, TX), overnight hybridization with the cDNA probe (25 ng) was carried out at 48°C. Abundance of hybridized mRNA was evaluated by autoradiography.

### Binding to solid-phase ICAM-1 by cotransfected COS-7 cells

As described previously<sup>13,15</sup> with modifications, flat-bottomed wells of 96-well microtiter plates (Immulon IV; Dynatech, Alexandria, VA) were coated overnight at 4°C with 3.0  $\mu$ g recombinant human intercellular adhesion molecule-1 (ICAM-1), washed, and blocked with 5% bovine serum albumin (BSA) for 1 hour at 37°C. After activation of COS-7 cells by treatment with the activating anti-CD18 mAb KIM185, COS-7 cells (10<sup>5</sup> in 0.1 mL) were added in triplicate to each well and allowed to settle onto the surface of the well for 15 minutes at 37°C. Nonadherent cells were carefully removed by 3 washes with phosphate-buffered saline (PBS). The number of cells retained at the bottom of each well was counted microscopically. Additional pretreatment of COS-7 cells with mAb R3.1 against LFA-1 ( $\alpha_L$ ) was used to confirm LFA-1 specificity of binding. The mean number of adherent cells in triplicate wells for KIM185-activated cells cotransfected with wild-type (wt)  $\beta_2$  was set at 100% for each separate experiment, and all other values were expressed as a percentage of that standard, calculated separately within each experiment.

### Rosetting of COS-7 cells with iC3b-coated sheep erythrocytes (iC3b-SRBCs)

An adaptation of previously described methods was employed.<sup>16-18</sup> Briefly, a 10% vol/vol suspension (0.3 mL) of SRBCs (ICN Biomedicals, Aurora, OH) was incubated for 60 minutes at 25°C with 30  $\mu$ g rabbit anti-SRBC immunoglobulin M (IgM; ICN Biomedicals). The IgM-coated SRBCs were washed, resuspended in C5-depleted human serum (Sigma-Aldrich, Dallas, TX) diluted to 25% in PBS, and incubated for 30 minutes at 37°C to permit opsonization of the IgM-SRBCs with iC3b. After thorough washing, approximately  $5 \times 10^7$  opsonized SRBCs were added to 10<sup>5</sup> COS-7 cells in a final volume of 150  $\mu$ L. These mixtures were centrifuged gently (150g for 3 minutes) to form a loose pellet then incubated at 37°C for 30 minutes. The pellets were resuspended and each suspension was examined by light microscopy for rosette formation, defined as 3 or more RBCs bound to one COS-7 cell (rosettes rarely contained fewer than 10 RBCs). An mAb against  $\alpha_M$  (clone 60.1) was used to confirm the Mac-1 specificity of rosetting.

### Assays for PMN adhesion and transendothelial migration

Suspensions of PMNs were injected into static adhesion chambers<sup>19,20</sup> and allowed to settle onto a coverslip coated with either keyhole limpet hemocyanin (KLH) or a monolayer of human umbilical vein endothelial cells (HUVECs), prepared as previously described.<sup>20</sup> After incubation at 37°C for 500 seconds, the chamber was inverted and nonadherent PMNs were allowed to settle onto an uncoated glass coverslip on the opposite side of the chamber. The percentage of PMNs that remained adherent to the substrate was determined by phase contrast microscopy. Of PMNs that were adherent to a HUVEC monolayer, those that traversed the endothelium were then distinguished by their flatter, "phase-dark" appearance, in contrast to the "phase-bright" appearance of PMNs that remained at the luminal surface of the monolayer.<sup>20</sup> PMN aggregation in response to 1.0  $\mu$ M fMLF was measured by the flow cytometric method of Rochon and Frojmovic.<sup>21</sup> In vivo migration of PMNs into skin suction blister fluid at successive time intervals was measured by adapting a previously described technique.<sup>22</sup>

### Chemiluminescence assay for PMN oxidative burst in response to opsonized zymosan particles

PMNs (10<sup>6</sup> cells in a final volume of 1.0 mL) were mixed in a cuvette at 37°C with 1 mg serum-opsonized zymosan particles, prepared as previously described,<sup>6,7</sup> and 10<sup>-5</sup> M lucigenin (bis-N-methyl acridinium nitrate).<sup>23</sup> At 5-minute intervals, the light that was emitted upon the reduction of lucigenin was measured in a temperature-controlled luminometer (model 1201; LKB-Wallac, Turku, Finland) and expressed in millivolts as a measure of PMN respiratory burst activation.<sup>23,24</sup> Mac-1 dependence was confirmed by blocking the receptor on PMNs with mAb 60.1. Phorbol myristate acetate (PMA) was used as a nonparticulate stimulus to confirm intrinsically normal respiratory burst activity.

## Results

### Analysis of patient's CD18 sequence data

A mutation was identified in the patient's CD18 sequence, characterized by a deletion of the last 36 nucleotides of exon 12 (1622del36; "A" of initiating ATG codon = 1). This deletion predicts a net loss of 12 amino acid (aa) residues in the third cysteine-rich repeat of the CD18 extracellular stalk region, with loss of 13 original aa residues and the insertion of a new tryptophan residue due to the formation of a new codon by nucleotides at the margins of deletion (C541\_G553delinsW).<sup>25</sup> This mutation, referred to below as "mut-1," is diagrammed in Figure 1A.

Returning to the patient's mononuclear cell RNA, additional PCR reactions using new primers closely flanking the above mutation yielded 2 distinct, equally intense product bands (data not shown), suggesting that the patient was heterozygous for this deletion. A second mutation was identified as a nonsense mutation in exon 15 (2200G>T), predicting a 36-aa truncation of the cytoplasmic domain of CD18 (E734X). This mutation, referred to below as "mut-2," is diagrammed in Figure 1B. The CD18 precursor, with designated locations of mut-1 and mut-2, is depicted in Figure 1C.

### Cell surface expression of LFA-1 and Mac-1 in COS-7 cells cotransfected with the wild-type (wt) $\alpha_L$ or $\alpha_M$ subunit in combination with the wt, mut-1, or mut-2 $\beta_2$ subunit

COS-7 cells cotransfected as described were analyzed for LFA-1 or Mac-1 expression by immunofluorescence flow cytometry. Fluorescence histograms for a representative set of transfections are shown in Figure 2. A composite of 4 similar experiments is represented in Figure 2B. Levels of expression of Mac-1 and LFA-1 were profoundly reduced for cells transfected with mut-1  $\beta_2$  versus wt  $\beta_2$ . In contrast, expression levels of Mac-1 and LFA-1 for cells transfected with mut-2  $\beta_2$  were equivalent to those for wt  $\beta_2$ . Message levels for both mut-1 and mut-2  $\beta_2$  subunits were equivalent to those for wt  $\beta_2$  by Northern analysis (Figure 2C), indicating that differences in  $\beta_2$  subunit transcription did not account for the observed differences in integrin expression. These results suggest that the portion of the CD18 stalk region deleted in mut-1 is essential for normal formation and surface expression of Mac-1 and LFA-1 heterodimers, whereas the portion of the cytoplasmic domain of  $\beta_2$  truncated in mut-2 has no discernable influence on Mac-1 or LFA-1 surface expression.

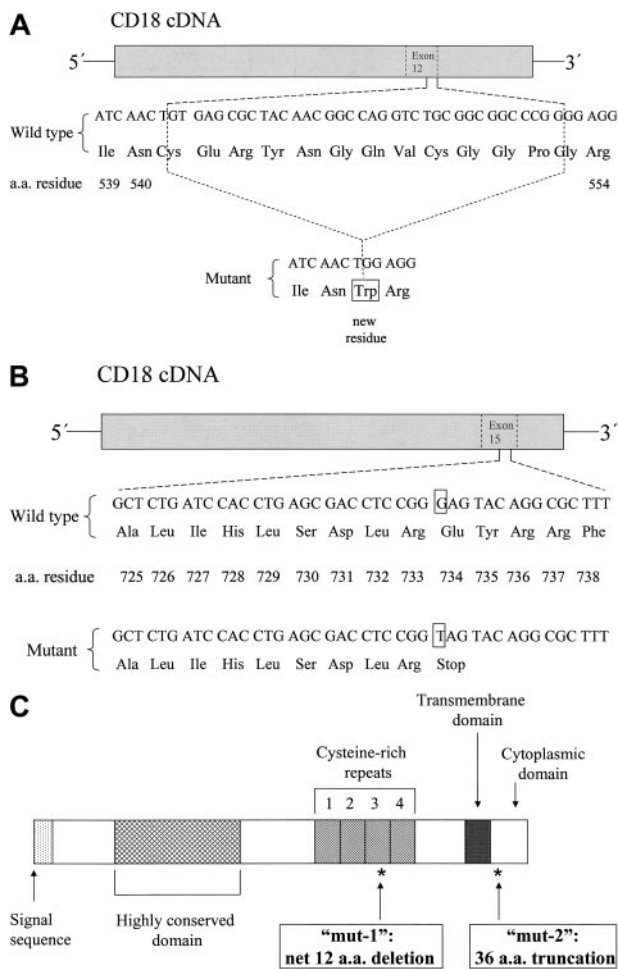


**Figure 1. Characterization of the patient's CD18 mutations.** The patient was determined to be a compound heterozygote with 2 distinct mutations. (A) A diagram of the first mutation defined, a 36–base pair deletion in exon 12 (1622del36), predicting a deletion of 13 aa residues and insertion of a new tryptophan residue (net loss of 12 aa residues) at the 3' end of the third cysteine-rich repeat domain of the CD18 extracellular stalk region (C541\_G553delinsW) and referred to in the text as "mut-1." (B) A diagram of the second mutation defined, a nonsense mutation creating a stop codon in exon 15 (2200G>T), predicting a 36-aa truncation of the CD18 cytoplasmic domain (E734X) and referred to in the text as "mut-2." A schematic diagram of the CD18 protein precursor is shown in panel C, including the locations of mut-1 and mut-2, as indicated by asterisks.

#### Adhesion of LFA-1–transfected COS-7 cells with wt, mut-1, and mut-2 $\beta_2$ to solid-phase ICAM-1

As shown in Figure 3A, adhesion to ICAM-1 in microtiter wells was profoundly reduced for  $\alpha_L$ -transfected COS-7 cells cotransfected with mut-1  $\beta_2$  compared with cells with wt  $\beta_2$ , concordant with the marked reduction in LFA-1 expression shown in Figure 2. Cells transfected with mut-2  $\beta_2$  showed a reduction in adhesion to ICAM-1 of approximately 50% compared with cells with wt  $\beta_2$ . All data shown are for cells pretreated with the activating mAb KIM185. Additional treatment with the anti- $\alpha_L$  mAb R3.1 confirmed the dependence on LFA-1 for adhesion in this assay. Untreated cells or cells treated with PMA instead of KIM185 exhibited low levels of adhesion, similar to untransfected or sham-transfected cells (not shown). These studies indicate that the

mut-2 cytoplasmic domain truncation of CD18 results in a significant reduction in LFA-1 function.

#### Rosetting of Mac-1–transfected COS-7 cells with IC3b-opsinized sheep erythrocytes

As shown in Figure 3B,  $\alpha_M$ -transfected COS-7 cells cotransfected with the mut-1  $\beta_2$  subunit formed very low numbers of rosettes compared with cells transfected with wt  $\beta_2$ , in keeping with very low Mac-1 surface expression levels. Rosetting of COS-7 cells cotransfected with mut-2  $\beta_2$  was equivalent to that with wt  $\beta_2$ . Additional treatment of the COS-7 cells with mAb 60.1 confirmed the Mac-1 dependence of rosetting. In contrast to the observed reduction in LFA-1 function associated with mut-2, these rosetting studies show that the mut-2 cytoplasmic domain truncation of CD18 does not interfere with Mac-1 function.

#### Surface expression of CD11/CD18 molecules on leukocytes from patient and family members compared with healthy controls

The average levels of CD18 integrin expression on the patient's leukocyte populations was 21% of healthy adult levels (Table 2). On unstimulated PMNs, CD11a was expressed at about 50% of normal levels and CD11b was approximately 17% of normal levels. A translocatable granular pool of CD11b in the patient's PMNs can be inferred from the 9-fold increase in CD11b surface levels after fMLF stimulation. CD11a and CD18 expression on the patient's peripheral blood lymphocytes ranged from 15% to 25% of control levels. Additional data not shown in the table include the following: (1) normal expression of L-selectin (CD62a), CR1 (CD35), and Fc $\gamma$ RII (CD32) on the patient's PMNs; (2) approximately 20% of control levels of CD11c expression on the patient's monocytes; (3) CD11b and CD18 expression for PMNs of both parents between 55% and 75% of control levels, consistent with their presumed status as obligate heterozygotes; (4) normal levels of CD11b and CD18 expression on PMNs from the patient's healthy sister; and (5) CD18 expression on the patient's EBV-transformed B lymphocytes of about 20% of control levels.

#### Adhesive functions of the patient's PMNs and the role of translocated Mac-1

The patient's PMNs exhibited marked reductions in adherence to KLH-coated glass and homotypic aggregation, the former a Mac-1–mediated process (Figure 4A and 4B, respectively). The patient's PMN oxidative burst in response to serum-opsinized zymosan was moderately reduced, with peak chemiluminescence values at 57% of control values (Figure 4C), and the response by both patient and control PMNs was reduced to baseline by the anti-Mac-1 mAb 60.1. Stimulation with PMA revealed an intrinsically normal respiratory burst mechanism (not shown).

Since previous studies have shown that newly translocated surface Mac-1 can also be activated for adhesion, we determined the extent of Mac-1–dependent adhesion by the patient's PMNs after graded chemoattractant-induced translocation of Mac-1. This analysis requires 2 sequential stimuli, one to mobilize Mac-1 to the cell surface followed by a second to activate adhesion via newly translocated Mac-1.<sup>14</sup> The patient's PMNs were first exposed to fMLF at suboptimal concentrations from 0.1 to 6.0 nM. Half of the cells from each condition were removed and stained to quantitate Mac-1 surface expression, and the other half were exposed to fMLF a second time at 10.0 nM and assayed for PMN adhesion to KLH-coated glass. As shown in Figure 5, with increasing concentrations of fMLF, there was a progressive increase both in surface

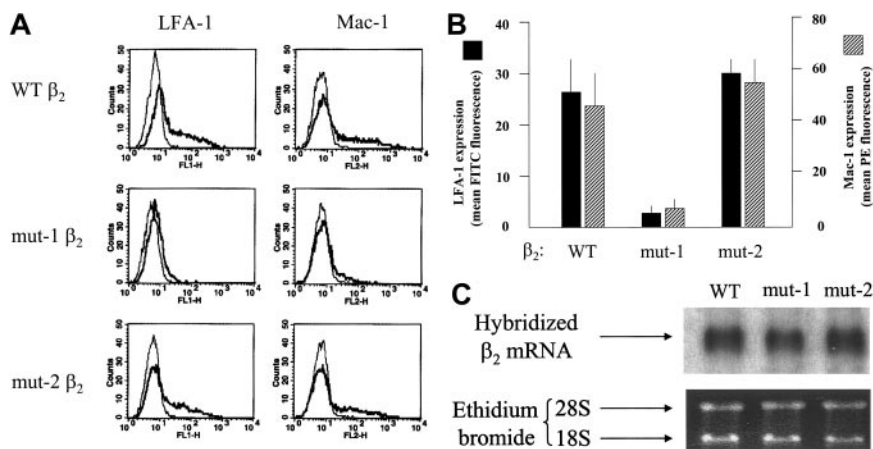


**Figure 2. Expression of LFA-1 and Mac-1 in COS-7 cells transiently cotransfected with the wild-type  $\alpha$  subunits of Mac-1 or LFA-1, plus the wt, mut-1, or mut-2  $\beta_2$  subunit.** (A) Fluorescence-activated cell sorter (FACS) histograms for expression of Mac-1 or LFA-1 on COS-7 cells cotransfected as indicated and stained with direct fluorescent conjugates of mAbs against the Mac-1 or LFA-1  $\alpha$  subunits or an isotype-matched control mAb. The thin lines represent background fluorescence with a control antibody, and the thick lines represent the specific fluorescence for LFA-1 or Mac-1. As shown, COS-7 cells transfected with the mut-1  $\beta_2$  subunit expressed markedly diminished Mac-1 and LFA-1 compared with cells with the wt  $\beta_2$ , whereas results with the mut-2  $\beta_2$  were similar to those for wild type. (B) A graph of the composite data from 4 such experiments, confirming the pronounced reduction in expression of Mac-1 and LFA-1 with the mut-1  $\beta_2$  subunit versus wt  $\beta_2$  ( $P < .001$ ;  $n = 5$ ). Error bars indicate SEM. Expression of Mac-1 and LFA-1 with the mut-2  $\beta_2$  was equivalent to their expression with wt  $\beta_2$ . RNA recovered from COS-7 cells transiently transfected as for the expression studies for panels A and B was subjected to Northern analysis as described in "Patients, materials, and methods." As shown in the autoradiogram in panel C, there was no apparent difference in mRNA abundance among the 3  $\beta_2$  mRNAs, confirming that the reduced expression of Mac-1 and LFA-1 with the mut-1  $\beta_2$  subunit could not be attributed to reduced transcription. The results shown are for RNA from COS-7 cells transfected with the respective  $\beta_2$  subunits along with the LFA-1  $\alpha$  subunit and represent 3 similar experiments.

expression of CD11b on the PMNs after the initial stimulus (Figure 5A) and in adherence by PMNs after the second fMLF stimulation (Figure 5B). When the relation between Mac-1 expression and percent PMN adherence for the patient's cells was analyzed by linear regression (Figure 5C), there was a strong direct relationship between adherence after the second stimulus and the number of Mac-1 sites on the cell surface prior to the second stimulus (regression coefficient  $[R] = 0.971$ ). Thus, the patient's PMN granular pool of Mac-1 can be activated for cell adhesion after translocation to the cell surface and that Mac-1 expressed on the patient's PMNs can bind to an appropriate ligand as effectively as wild-type Mac-1, consistent with the above rosetting data with COS-7 cells expressing Mac-1 with the patient's mut-2  $\beta_2$  subunit.

**Adhesion by the patient's PMNs to activated HUVEC monolayers, transendothelial migration in vitro, and the effects of blocking mAbs**

As shown in Figure 6, the adhesion of the patient's PMNs to cytokine-activated endothelium was markedly higher than to protein-coated glass (Figure 4A) but transmigration was low. This is consistent with earlier data indicating that transendothelial migration is largely CD11/CD18 dependent, while adhesion, per se, can be mediated by other molecules as well, including PMNs and endothelial selectins.<sup>20,26</sup> When E-selectin on endothelial cells was blocked with mAb CL2, adhesion by the patient's PMNs to the HUVECs was reduced by

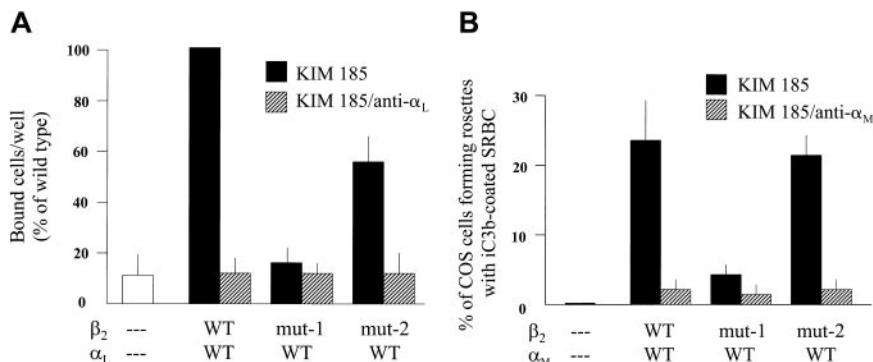


**Figure 3. Adhesion to solid-phase purified ICAM-1 or rosetting with iC3b-opsioned sheep RBCs (SRBCs) by cotransfected COS-7 cells.** COS-7 cells transfected with the wt, mut-1, or mut-2  $\beta_2$  subunit plus the wt LFA-1  $\alpha$  subunit (A) were activated with the KIM185 mAb and added ( $10^5$  cells) to triplicate ICAM-1-coated microtiter wells for 15 minutes at 37°C. After removing nonadherent cells by 3 gentle PBS washes, the number of cells retained in each well was directly counted by microscopy (see Figure 2). The mean value for LFA-1/wt $\beta_2$  cells was set at 100% for each experiment, and all other values for that experiment were expressed as a percentage of that standard. As shown, binding to ICAM-1 by cells transfected with mut-1  $\beta_2$  was no different than the background level observed for untransfected cells, consistent with nearly absent LFA-1 expression (see Figure 2). Binding by cells expressing LFA-1 with mut-2  $\beta_2$  was diminished by about 50% compared with wt  $\beta_2$  ( $P < .05$ ;  $n = 4$ ), indicating diminished functional activity of LFA-1 containing mut-2  $\beta_2$ . Treatment with mAb R3.1 after activation with KIM185 completely abrogated binding to ICAM-1, confirming the LFA-1 dependence of binding. (B) SRBCs opsonized with iC3b as described in "Patients, materials, and methods" ( $5 \times 10^7$  cells) were mixed with COS-7 cells that had been transfected with the wt Mac-1  $\alpha$  subunit plus the wt, mut-1, or mut-2  $\beta_2$  subunit ( $10^5$  COS-7 cells). After 30-minute incubation at 37°C, as described, the cell mixtures were examined by light microscopy for rosette formation, defined as at least 3 SRBCs bound to one COS-7 cell. As shown, COS-7 cells transfected with mut-1  $\beta_2$  exhibited very low levels of rosetting compared with cells transfected with wt  $\beta_2$ . In contrast, COS-7 cells transfected with mut-2  $\beta_2$  formed rosettes to the same extent as cells transfected with wt  $\beta_2$ , indicating that the mut-2  $\beta_2$  subunit had no effect on Mac-1-mediated binding. Treatment of COS-7 cells with mAb 60.1 after activation with KIM185 virtually abrogated rosetting, confirming the Mac-1 dependence of this function. Error bars indicate SEM.

**Table 2. Representative data for expression of CD18 integrins determined by immunofluorescence flow cytometry of PMN and lymphocyte subsets (CD3<sup>+</sup>, CD4<sup>+</sup>, CD8<sup>+</sup>) in whole blood of the patient and a healthy adult control**

Antigen	Source*	PMNs	PMN/fMLF†	CD3 <sup>+</sup>	CD4 <sup>+</sup>	CD8 <sup>+</sup>
CD18	C	128‡	572	1632	1262	1953
CD18	P	41	131	236	300	437
CD11a	C	63	75	760	542	890
CD11a	P	32	41	110	137	127
CD11b	C	314	2115	—	—	—
CD11b	P	54	510	—	—	—

— indicates marker not assayed.

\*Blood from the adult control (C) or the patient (P).

†fMLF (10 nM) was added to stimulate translocation of stored CD11b/CD18 to the PMN surface.

‡Value for mean fluorescence intensity, using directly conjugated mAbs to each subunit antigen.

about 50% (not shown), confirming the participation of selectins in this process.

As previously reported for control PMNs,<sup>20</sup> blocking CD18 almost completely inhibited transendothelial migration for both patient and control PMNs (Figure 7). For control PMNs, blocking CD11b had a relatively small inhibitory effect compared with blocking CD11a, also consistent with previous data.<sup>20</sup> However, transmigration of the patient's cells was blocked by mAbs to either CD11a or CD11b as effectively as by anti-CD18. It seems likely that CD11a and CD11b expression is sufficiently low on the patient's cells that blocking either one abrogates transmigration. Accumulation of the patient's PMNs in skin suction blister fluid by 6 hours after blister induction was approximately 30% of adult control values (data not shown), similar to the above comparisons for transmigration.

## Discussion

One of the current patient's CD18 mutations (mut-1) was a deletion of 36 nucleotides in exon 12, predicting a deletion of 13 aa residues and the insertion of a tryptophan residue (C541\_G553delinsW), a net loss of 12

aa residues. This deletion in the third cysteine-rich repeat domain of the extracellular stalk region eliminates 2 cysteine residues at positions 541 and 549 that participate in disulfide bonds important for CD18 tertiary structure.<sup>27</sup> The extracellular stalk region of CD18 has been shown to be important for effective integrin heterodimer formation, and the cysteine-rich repeats near the carboxy-terminal end of the stalk region contain epitopes that define conformational changes critical for activation of alpha subunit binding.<sup>27,28</sup> Two previous studies concluded that the "major cysteine-rich region" is not required for Mac-1 or LFA-1 surface expression.<sup>28,29</sup> However, the patient's mut-1 deletion results in very low levels of surface expression of both LFA-1 and Mac-1, suggesting that specific deletions in this region can alter the CD18 structure sufficiently to cause a profound impairment of integrin heterodimer formation and expression, presumably resulting in intracellular degradation of most monomeric subunits that do not form heterodimers, as reviewed previously.<sup>1</sup> Northern analysis of CD18 mRNA in transfected COS cells revealed that the low surface expression of Mac-1 and LFA-1 with mut-1 was not accounted for by reduced transcription. PCR studies with RNA from the patient's mononuclear cells and primers closely flanking the mut-1 deletion initially revealed the patient's status as a compound heterozygote, based on the presence of 2 distinct, equally intense bands from the same reaction and, while not quantitatively definitive, suggested no selective advantage for either mut-1 or the alternate allele, mut-2, at the RNA level. The very low ligand binding by LFA-1- and Mac-1-transfected COS-7 cells that contained the mut-1  $\beta_2$  subunit were in keeping with the low levels of cell surface expression.

The patient's second mutation (mut-2) was a nonsense mutation in exon 15, predicting a 36-aa truncation of the CD18 cytoplasmic domain (E734X). To our knowledge, this is the first reported CD18 mutation associated with LAD-1 that specifically involves the cytoplasmic domain. Progressive truncations of the CD18 cytoplasmic domain produced by site-directed mutagenesis have not appeared to have significant effects on CD18 integrin cell surface expression,<sup>13</sup> and our studies showing equivalent expression of Mac-1 or LFA-1 in cotransfected COS-7 cells with the patient's mut-2 compared with wt  $\beta_2$  were consistent with those findings. The current results might suggest that expression of Mac-1 and LFA-1 on the patients circulating leukocytes should approach 50%

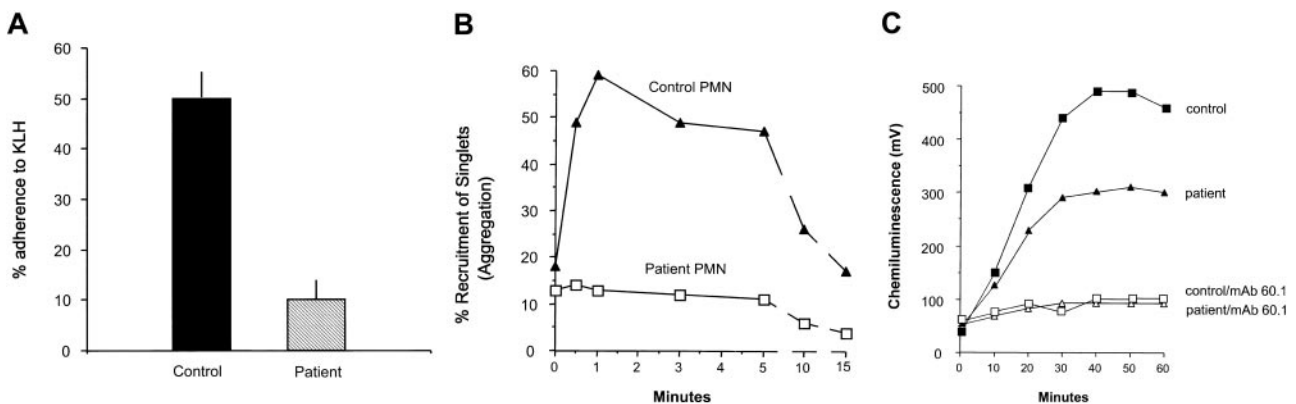


**Figure 4. Stimulated adherence to KLH-coated glass, homotypic aggregation, and oxidative burst in response to opsonized zymosan particles by patient versus control neutrophils.** (A) Neutrophils stimulated with 10 nM fMLF were assayed for adherence to KLH-coated coverslips in adhesion chambers as described. Results are expressed as the percentage of neutrophils that adhered to the KLH-coated surface (% adherence). Error bars indicate SEM. The patient's values are diminished to about 20% of those for control ( $P < .05$ ;  $n = 3$ ). Homotypic aggregation (B), measured as the recruitment of single neutrophils into doublets, triplets, and larger aggregates (% recruitment of singlets) was measured by flow cytometry of fixed aliquots from a stirring suspension of neutrophils at successive time intervals after addition of 1.0  $\mu$ M fMLF. Markedly impaired aggregation was observed for the patient's cells compared with controls. Two additional assays yielded similar results. The patient's neutrophils were compared with those from a healthy adult control in an assay that measured the oxidative burst of the cells in response to iC3b-opsonized zymosan particles, using a lucigenin-dependent chemiluminescence assay that measures superoxide release (C). The patient's cells exhibited a moderately reduced oxidative burst in response to opsonized zymosan particles compared with the other subjects, with the area under the chemiluminescence (CL) curve for the patient achieving approximately 57% of the control value. Treatment of PMNs with the anti-Mac-1 mAb 60.1 virtually eliminated the response to opsonized zymosan for both patient and control PMNs. Two additional experiments comparing the patient's neutrophils with those from a healthy control yielded similar results.

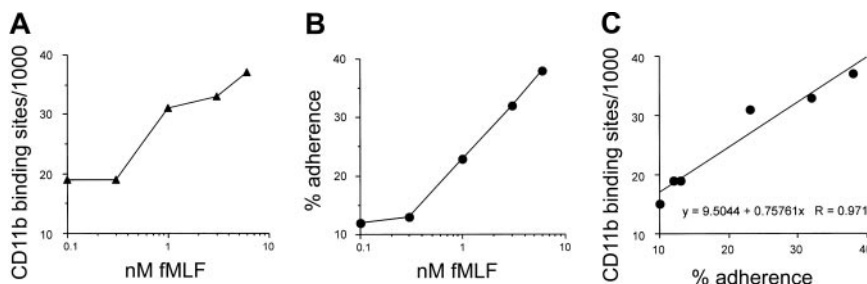


**Figure 5. Relationship between neutrophil Mac-1 surface expression and stimulated Mac-1–dependent adherence to KLH-coated glass for the patient’s PMNs.** As described in “Patients, materials, and methods,” neutrophils from the patient were treated with a range of suboptimal concentrations of fMLF from 0.1 to 6.0 nM. Cells from each stimulation condition were divided into 2 separate aliquots, and one was stained to quantitate Mac-1 surface sites (A). The other was subjected to a second fMLF stimulation at 10 nM, then assayed for % adherence to KLH-coated glass (B). (C) The strong quantitative relationship by linear regression analysis ( $R = 0.971$ ) between the number of Mac-1 sites before the second stimulus and % adherence after the second stimulus.

of normal levels. However, as noted in Table 2, the patient’s values were in the range of 15% to 25% of normal levels (only LFA-1 on the patient’s PMNs approached 50% of control levels), suggesting that the regulation of Mac-1 and LFA-1 expression in native leukocytes differs from that in transfected COS-7 cells. Because surface expression of these integrins with mut-1 in COS-7 cells is almost negligible, it seems reasonable to suggest that nearly all of the Mac-1 and LFA-1 expressed on the patient’s native cells contain the mut-2  $\beta_2$  subunit.

The CD18 cytoplasmic domain engages in important interactions with the cytoskeleton and appears to regulate several important aspects of  $\beta_2$  integrin function and trafficking. Important binding sites for talin,  $\alpha$ -actinin, and filamin, as well as a distinct site inhibitory for  $\alpha$ -actinin binding, are among relevant sites present on the cytoplasmic domain of CD18.<sup>30,31</sup> Such sites appear to be critical for regulating the engagement and disengagement of the  $\beta_2$  integrins with the cytoskeleton and are, thus, important for regulating cell orientation, spreading on surfaces, and directed migration.<sup>1,32</sup> Phosphorylation of CD18 occurs at several distinct sites in the cytoplasmic domain and may regulate integrin functions, including cytoskeletal association.<sup>33–35</sup> One or more isoforms of protein kinase C may phosphorylate S745, S756, T758, or T760,<sup>34,35</sup> although the functional significance of phosphorylation at each of these sites is not fully understood. A tyrosine-based sorting signal, YRRF at Y735, seems important for recycling of internalized integrins to the cell surface and ligand-supported migration in transfected Chinese hamster ovary (CHO) cells.<sup>36</sup> All of the above-mentioned sites are eliminated by the patient’s mut-2 truncation mutation. Studies involving progressive truncations of the CD18 cytoplasmic domain by site-directed mutagen-

esis have shown that even small truncations of this domain may lead, in transfected COS-7 cells, to dramatic reductions in binding by LFA-1 to ICAM-1.<sup>13</sup> The longest CD18 truncation produced in the aforementioned studies, with the loss of 39 aa residues (vs 36 residues for the mut-2 truncation in our patient), resulted in higher levels of LFA-1–dependent binding to ICAM-1 than did shorter truncations, although binding was still about 30% less than with wt CD18.

COS-7 cells expressing LFA-1 with the patient’s mut-2  $\beta_2$  subunit were significantly impaired, versus wt  $\beta_2$ , in binding to solid-phase ICAM-1, despite equivalent surface expression of LFA-1. In contrast, COS-7 cells expressing Mac-1 with mut-2  $\beta_2$  formed rosettes with iC3b-SRBCs equally as well as COS-7 cells expressing Mac-1 with wt  $\beta_2$ . Thus, as has been suggested previously,<sup>29</sup> the  $\beta_2$  cytoplasmic domain may influence LFA-1 function in a manner distinct from Mac-1 function. This idea is difficult to address definitively in the patient’s native leukocytes that may exhibit reductions in both LFA-1 function and LFA-1 expression. However, the COS-7 cell data are consistent with the suggestion that the reduced transendothelial migration of the patient’s PMNs, a function supported predominantly by LFA-1,<sup>20</sup> is due to both diminished function and diminished expression of LFA-1. Overall, our findings with COS-7 cells suggest that the principal contribution of mut-1 to the overall LAD-1 phenotype is greatly reduced integrin surface expression, whereas that of mut-2 is a reduction of LFA-1 adhesive function without affecting the function of Mac-1.

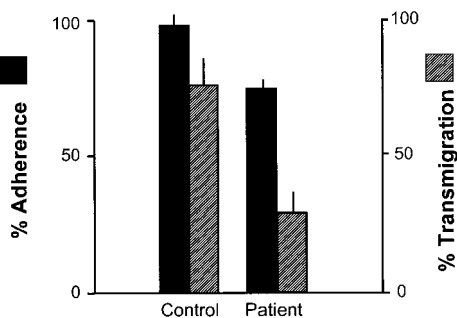


**Figure 6. Adherence to cultured endothelial monolayers and transendothelial migration by patient and control neutrophils.** Endothelial monolayers (HUVECs) prepared as described were overlaid with neutrophils in adhesion chambers. After 500 seconds, % adherence to the monolayers was determined. After 1000 seconds, the proportion of adherent neutrophils that migrated across the monolayers was determined by phase contrast microscopy. Adherence of the patient’s neutrophils in this system was modestly impaired compared with controls but transendothelial migration was severely impaired ( $P < .05$ ;  $n = 3$ ), consistent with the CD11/CD18 dependence of the latter process. Error bars indicate SEM.

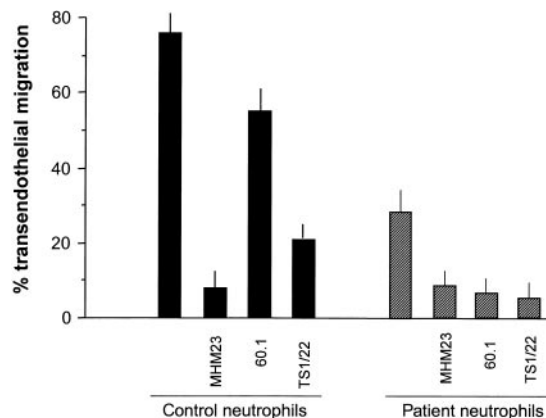


**Figure 7. Effects of blocking CD11/CD18 subunits on the transendothelial migration of patient versus control neutrophils.** Neutrophils were treated with saturating concentrations of mAbs against CD18 (MHM23), CD11a (TS1/22), and CD11b (60.1) or a control cell-binding mAb before evaluating transendothelial migration (TEM) as described earlier. As for Figure 6, TEM by the patient’s neutrophils was markedly diminished compared with controls. For control neutrophils, blocking CD18 almost completely inhibited TEM, and blocking CD11a also markedly reduced TEM. However, blocking CD11b produced only a modest inhibition. For patient neutrophils, all 3 mAbs produced virtually complete inhibition of TEM. Error bars indicate SEM.

That Mac-1–dependent binding (rosetting) was equivalent for COS-7 cells cotransfected with mut-2 versus wt  $\beta_2$  (Figure 3B) also found a parallel in studies with the patient's native PMNs. It is well established that stimulated Mac-1–dependent adhesion by PMNs is mediated by Mac-1 present on the cell surface at the time of stimulation.<sup>37-39</sup> However, as demonstrated by Hughes et al,<sup>14</sup> translocated Mac-1 can also be activated for adhesion and migration by subsequent stimuli. We found that treatment of our patient's PMNs with a graded range of suboptimal stimuli (up to 6 nM fMLF) resulted in incremental increases in Mac-1 surface expression (Figure 5A), with Mac-1 expression after treatment with 6 nM fMLF being similar to that on unstimulated control PMNs (Table 1). When a second stimulus (10 nM fMLF) was applied to these PMNs, the level of adhesion to KLH-coated glass also increased with the concentration of the first stimulus (Figure 5B). For the 6 nM/10 nM fMLF sequential stimulation, adhesion to KLH was roughly equivalent to the adhesion observed for control PMNs after a single stimulus with 10 nM fMLF shown in Figure 4A. Taken together with our findings in transfected COS-7 cells, these results indicate that the patient's PMN Mac-1, including that translocated from storage compartments, is as effective as wild-type Mac-1 in ligand binding. Studies by Buyon et al<sup>40</sup> indicating that phosphorylation of Mac-1 occurs at the plasma membrane but not in specific granule membranes showed further that chemoattractant stimulation (fMLF) resulted in phosphorylation of only the  $\alpha_M$  subunit and not the  $\beta_2$  subunit. This is consistent with our findings of normal activation of the patient's PMN Mac-1 by fMLF stimulation, in that loss of most of the  $\beta_2$  cytoplasmic domain might be predicted to have no discernible effect under these conditions.

PMN adhesion after the second stimulus in the above model of sequential fMLF stimulation was directly proportional to the number of Mac-1 sites present on the cell surface after the initial stimulus ( $R = 0.971$  by linear regression). Such a quantitative relationship would have been more difficult to establish in control PMNs because the level of Mac-1–dependent adhesion to KLH following a single 10 nM fMLF stimulus is already nearly 50%, and even after a 5- to 6-fold up-regulation of Mac-1 surface expression by an initial stimulus, the range available for increased adherence to KLH after a second stimulus would be limited to less than 2-fold. The findings with the patient's cells would appear to

show that the amount of Mac-1 on the PMN surface at the time of a given chemoattractant stimulus, whether resident surface Mac-1 or Mac-1 previously translocated to the PMN surface, is directly proportional to the capacity for Mac-1–dependent ligand binding induced by that stimulus.

The patient considered here is unique as the only example known to us of LAD-1 associated with a mutation that specifically involves the CD18 cytoplasmic domain. He also exhibits one clinical feature that is, to our knowledge, unique among patients with LAD-1 in that he tends to form hypertrophic scars after skin injury rather than the atrophic scars observed in other patients with LAD-1.<sup>1,7</sup> It remains to be determined if there is a link between these 2 unique features and if the CD18 cytoplasmic domain may play a role in regulating wound healing. Infiltrating leukocytes are an important feature of healing wound tissue, and PMNs, lymphocytes, and macrophages may be sources of transforming growth factor  $\beta$  (TGF $\beta$ ), a growth factor important in the activity of fibroblasts in healing wounds.<sup>41-46</sup> However, the role of leukocytes in wound healing is complex, and they may function both to promote or retard wound healing or scar formation, depending on the timing and circumstances related to a given injury.<sup>41,43,44</sup> Confirmation of a link between scarring and CD18 cytoplasmic domain function may be tested in transgenic mice expressing this patient's CD18 truncation.

One historic issue deserves comment. The above-cited 1979 report involving this patient<sup>8</sup> implicated the overgrowth of *Capnocytophaga* in the oral cavity in the pathogenesis of PMN chemotactic dysfunction before LAD-1 was a recognized disorder. The documentation of LAD-1 in this patient should encourage a reassessment of this clinical association. Since the PMN granule protease cathepsin G has been found to be a critical constituent in killing of *Capnocytophaga*,<sup>47</sup> it seems likely that impaired delivery of PMNs to gingival tissue would be the cause rather than the consequence of the overgrowth of this organism.

## Acknowledgments

The authors wish to thank Leo Mendoza for assistance with analysis of DNA sequence data, Dr David Kaplan for preparation of lymphocyte lines, and Bonnie J. Hughes for expert technical assistance.

## References

- Anderson DC, Smith CW. Leukocyte adhesion deficiencies. In: Scriver C, Beaudet A, Sly W, Valle D, eds. *The Metabolic and Molecular Basis of Inherited Disease*. 8th ed. New York, NY: McGraw-Hill; 2001:4829-4856.
- Springer TA, Anderson DC. Leukocyte complement receptors and adhesion proteins in the inflammatory response: insights from an experiment of nature. *Biochem Soc Symp*. 1986;51:47-57.
- Mathew EC, Shaw JM, Bonilla FA, Law SKA, Wright DA. A novel point mutation in CD18 causing the expression of dysfunctional CD11/CD18 leukocyte integrins in a patient with leukocyte adhesion deficiency (LAD). *Clin Exp Immunol*. 2000; 121:133-138.
- Hogg N, Stewart MP, Scarth SL, et al. A novel leukocyte adhesion deficiency caused by expressed but nonfunctional  $\beta_2$  integrins Mac-1 and LFA-1. *J Clin Invest*. 1999;103:193-202.
- Roos D, Meischl C, deBoer M, et al. Genetic analysis of patients with leukocyte adhesion deficiency: genomic sequencing reveals otherwise undetectable mutations. *Exp Hematol*. 2002;30: 252-261.
- Anderson DC, Schmalstieg FC, Arnaout MA, et al. Abnormalities of polymorphonuclear leukocyte function associated with a heritable deficiency of high molecular weight surface glycoproteins (GP138): common relationship to diminished cell adherence. *J Clin Invest*. 1984;74:536-551.
- Anderson DC, Schmalstieg FC, Finegold MJ, et al. The severe and moderate phenotypes of heritable Mac-1, LFA-1 deficiency: their quantitative definition and relation to leukocyte dysfunction and clinical features. *J Infect Dis*. 1985;152:668-689.
- Shurin SB, Socransky SS, Sweeney E, Stossel TP. A neutrophil disorder induced by *Capnocytophaga*, a dental micro-organism. *N Engl J Med*. 1979;301:849-854.
- Abbassi O, Kishimoto TK, McIntire L, Anderson DC, Smith CW. E-selectin supports neutrophil rolling in vitro under conditions of flow. *J Clin Invest*. 1993;92:2719-2730.
- Abughali N, Berger M, Tosi MF. Diminished total cell content of CD11b/CD18 in polymorphonuclear leukocytes of newborn infants. *Blood*. 1994;83:1086-1092.
- Robinson J, Smith D. Infection of human B-lymphocytes with high multiplicity of Epstein-Barr virus: kinetics of EBNA expression, cellular DNA synthesis, and mitosis. *Virology*. 1981;109:336-343.
- Weitzman JB, Wells CE, Wright AH, Clark PA, Law SK. The gene organization of the human beta 2 integrin subunit (CD18). *FEBS Lett*. 1991; 294:97-103.
- Hibbs ML, Xu H, Stacker SA, Springer TA. Regulation of adhesion to ICAM-1 by the cytoplasmic domain of LFA-1 integrin  $\beta$  subunit. *Science*. 1991;261:1611-1613.
- Hughes BJ, Hollers JC, Crockett-Torabi E, Smith CW. Recruitment of CD11b/CD18 to the neutrophil surface and adherence-dependent cell locomotion. *J Clin Invest*. 1992;90:1687-1696.
- Hibbs ML, Jakes S, Stacker SA, Wallace RW, Springer TA. The cytoplasmic domain of the integrin lymphocyte function-associated antigen-1  $\beta$  subunit: sites required for binding to intercellular adhesion molecule-1 and the phorbol ester-stimulated phosphorylation site. *J Exp Med*. 1991;174:1227-1238.
- Berger M, O'Shea J, Cross AS, et al. Human neutrophils increase expression of C3bi as well as C3b receptors upon activation. *J Clin Invest*. 1984;74:1566-1571.
- Diamond MS, Garcia-Aguilar J, Bickford JK, Corbi AL, Springer TA. The I domain is a major recognition site on the leukocyte integrin Mac-1



- (CD11b/CD18) for four distinct adhesion ligands. *J Cell Biol.* 1993;120:1031-1043.
18. McGuire SL, Bajt ML. Distinct ligand binding sites in the I domain of integrin  $\alpha$ Mb2 that differentially affect a divalent cation-dependent conformation. *J Biol Chem.* 1995;270:25866-25871.
  19. Smith CW, Hollers JC, Patrick RA, Hassett C. Motility and adhesiveness in human neutrophils: effects of chemotactic factors. *J Clin Invest.* 1979;63:221-229.
  20. Smith CW, Marlin SD, Rothlein R, Toman C, Anderson DC. Cooperative interactions of LFA-1 and Mac-1 with intercellular adhesion molecule-1 in facilitating adherence and transendothelial migration of human neutrophils in vitro. *J Clin Invest.* 1989;83:2008-2017.
  21. Rochon YP, Frojmovic MM. Dynamics of human neutrophil aggregation evaluated by flow cytometry. *J Leukoc Biol.* 1991;50:434-443.
  22. Kuhns DB, DeCarlo E, Hawk DM, Gallin JI. Dynamics of the cellular and humoral components of the inflammatory response elicited in skin blisters in humans. *J Clin Invest.* 1992;89:1734-1740.
  23. Minkenberg I, Ferber E. Lucigenin-dependent chemiluminescence as a new assay for NADPH oxidase activity in particulate fractions of human polymorphonuclear leukocytes. *J Immunol Methods.* 1984;71:61-67.
  24. Tosi M, Hamedani A. A rapid, specific assay for superoxide release from phagocytes in small volumes of whole blood. *Am J Clin Pathol.* 1992;97:566-573.
  25. den Dunnen JT, Antonarakis SE. Nomenclature for the description of human sequence variations. *Hum Genet.* 2001;109:121-124.
  26. Smith CW, Kishimoto TK, Abassi O, et al. Chemotactic factors regulate lectin adhesion molecule-1 (LECAM-1) dependent neutrophil adhesion to cytokine-stimulated endothelial cells in vitro. *J Clin Invest.* 1991;87:609-618.
  27. Beglova N, Blacklow SC, Takagi J, Springer TA. Cysteine-rich module structure reveals a fulcrum for integrin rearrangement upon activation. *Nat Struct Biol.* 2002;9:282-287.
  28. Douglass WA, Hyland RH, Buckley CD, et al. The role of the cysteine-rich region of the  $\beta_2$  integrin subunit in the leukocyte function-associated antigen-1 (LFA-1,  $\alpha_L\beta_2$ , CD11a/CD18) heterodimer formation and ligand binding. *FEBS Lett.* 1998;440:414-418.
  29. Tan S-M, Hyland RH, Al-Shamkhani A, Douglass WA, Shaw JM, Law SKA. Effect of integrin  $\beta_2$  subunit truncation on LFA-1 (CD11a/CD18) and Mac-1 (CD11b/CD18) assembly, surface expression, and function. *J Immunol.* 2000;165:2574-2581.
  30. Sampath R, Gallagher PJ, Pavalko FM. Cytoskeletal interactions with the leukocyte integrin  $\beta_2$  cytoplasmic tail: activation-dependent regulation of associations with talin and alpha-actinin. *J Biol Chem.* 1998;273:33588-33594.
  31. Sharma CP, Ezzell RM, Amaout MA. Direct interaction of filamin (ABP-280) with the beta 2-integrin subunit CD18. *J Immunol.* 1995;154:3461-3470.
  32. Pavalko FM, Otey CA. Role of adhesion molecule cytoplasmic domains in mediating interaction with the cytoskeleton. *Proc Soc Exp Biol Med.* 1994;205:282-293.
  33. Valmu L, Fagerholm S, Suila H, Gahmberg CG. The cytoskeletal association of CD11/CD18 leukocyte integrins in phorbol ester-activated cells correlates with CD18 phosphorylation. *Eur J Immunol.* 1999;29:2107-2118.
  34. Fagerholm S, Morrice N, Gahmberg CG, Cohen P. Phosphorylation of the cytoplasmic domain of the integrin CD18 chain by protein kinase C isoforms in leukocytes. *J Biol Chem.* 2002;277:1728-1738.
  35. Valmu L, Hilden TJ, van Willigen G, Gahmberg CG. Characterization of  $\beta_2$  (CD18) integrin phosphorylation in phorbol ester-activated T lymphocytes. *Biochem J.* 1999;339:119-125.
  36. Fabbri M, Fumagalli L, Bossi G, Bianchi E, Bender JR, Pardi R. A tyrosine-based sorting signal in the  $\beta_2$  integrin cytoplasmic domain mediates its recycling to the plasma membrane and is required for ligand-supported migration. *EMBO J.* 1999;18:4915-4925.
  37. Vedder NB, Harlan JM. Increased surface expression of CD11b/CD18 (Mac-1) is not required for stimulated adherence to cultured endothelium. *J Clin Invest.* 1988;81:676-682.
  38. Philips MR, Buyon JP, Winchester R, Weissman GH, Abramson SB. Up-regulation of the iC3b receptor is neither necessary nor sufficient to promote neutrophil aggregation. *J Clin Invest.* 1988;82:495-501.
  39. Diamond MS, Springer TA. A subpopulation of Mac-1 (CD11b/CD18) molecules mediates neutrophil adhesion to ICAM-1 and fibrinogen. *J Cell Biol.* 1993;120:545-556.
  40. Buyon JP, Philips MR, Merrill JT, Slade SG, Leszczynska-Piziak J, Abramson SB. Differential phosphorylation of the  $\beta_2$  integrin CD11b/CD18 in the plasma and specific granule membranes of neutrophils. *J Leukoc Biol.* 1997;61:313-321.
  41. Boyce DE, Ciampolini J, Ruge F, Murison MS, Harding KG. Inflammatory cell populations in keloid scars. *Br J Plast Surg.* 2001;54:511-516.
  42. Boyce DE, Jones WD, Ruge F, Harding KG, Moore KI. The role of lymphocytes in human dermal wound healing. *Br J Dermatol.* 2000;143:59-65.
  43. DiPietro LA. Wound healing: the role of macrophages and other immune cells. *Shock.* 1995;4:233-240.
  44. Dovi JV, He LK, DiPietro LA. Accelerated wound closure in neutrophil depleted mice. *J Leukoc Biol.* 2003;73:448-455.
  45. Chircop MP, Yu Y, Bereney CR, Yang JL, Crowe PJ, Walsh WR. Wound healing and growth factor expression in T lymphocyte deficiency. *ANZ J Surg.* 2002;72:491-495.
  46. Ahuja SS, Shrivastav S, Danielpour D, Balow JE, Boumpas DT. Regulation of transforming growth factor-beta 1 and its receptor by cyclosporine in human lymphocytes. *Transplantation.* 1995;60:718-723.
  47. Miyasaki KT, Bodeau AL. In vitro killing of oral *Capnocytophaga* by granule fractions of human neutrophils associated with cathepsin G activity. *J Clin Invest.* 1991;87:1585-1593.